Int J Adv Manuf Technol (2017) 88:1557–1565
DOI 10.1007/s00170-016-8873-0

ORIGINAL ARTICLE

# The investigation of laser shock peening effects on corrosion and hardness properties of ANSI 316L stainless steel

**Mohammad Ebrahimi**[1] · **Saeid Amini**[1] · **Seyed Mohammad Mahdavi**[2,3]

Received: 7 November 2015 / Accepted: 3 May 2016 / Published online: 16 May 2016


**Abstract** Laser shock peening (LSP) is known as a post processing surface treatment which can improve the mechanical properties of some materials. Shock waves are generated by confining the laser-induced plasma to cause a large pressure shock wave over a significant surface area. In the present study, effects of LSP on the electrochemical corrosion and micro hardness properties of 316L stainless steel alloy were investigated by changing the laser parameters such as the laser spot size, the average number of impacts, and the laser intensity. Since laser parameters do not cover the desired region of LSP, we have to use the proper design of experiment method, in which the D-optimal design of MATLAB was selected. Results revealed that by increase in irradiance, number of impacts and spot size of laser beam, improvement in the surface micro hardness, and corrosion resistance is achieved. Also, due to unexpected drop into the outcome of our experiments, it was found that the contamination of the transparent overlay and reduction of the absorption coefficient of the absorbent layer play a key role to reduce the efficiency of the mechanical impacts. So, by changing the experimental conditions, even better results are expected.

**Keywords** Laser shock peening · Corrosion · Micro hardness · 316L stainless steel · D-optimal design

✉ Saeid Amini
Amini.s@kashanu.ac.ir

[1] Manufacturing Department, Faculty of Mechanical Engineering, University of Kashan, Kashan, Iran

[2] Department of Physics, Sharif University of Technology, Tehran, Iran

[3] Institute for Nanoscience and Nanotechnology, Sharif University of Technology, Tehran, Iran

## 1 Introduction

In this study, the LSP technique, as a post processing step, is investigated. The absorption of pulsed laser by material lead to a plume right on the surface (which is pressurized plasma (ionized gas)). Confinement of the generated plasma can produce shock waves and compression stress through the material from surface to the depth. This mechanical impulse can improve mechanical properties and the operation of the material. A schematic configuration of LSP process is shown in Fig. 1. Improvement of the mechanical properties of the material, using LSP process, can be seen in the literature [1]. Gas power plant turbines are good examples of improved operations in this technique, because they are subjected to many wearing factors such as corrosion, erosion, and fatigue.

After LSP technique became known in early 1960s, other mechanisms were established to improve the LSP process. So, after adding transparent overlay and absorbing coating, this process reached its maturity in 80s.

In 2008, Warren et al. used FEA simulation and compared with measured data to determine the effects of laser intensity, laser spot size, and peening spacing on stress and strain fields [2].

In 2009, Vukelic et al. investigated the grain boundary response after LSP of aluminum. In order to investigate heterogeneity, the grain boundary is shocked, and to study the effect of anisotropy in the absence of heterogeneity, the single crystals are shocked. Then, comparing simulation results with experimental findings led to the potential benefit of improvement of fatigue life for $\mu LSP$ [3].

In 2009, Hatumleh made a comprehensive investigation on the effects of LSP on fatigue crack growth in friction stir welded samples. The results showed a significant improvement in fatigue crack growth rates of LSP in comparison with shot peened and native welded samples [4].

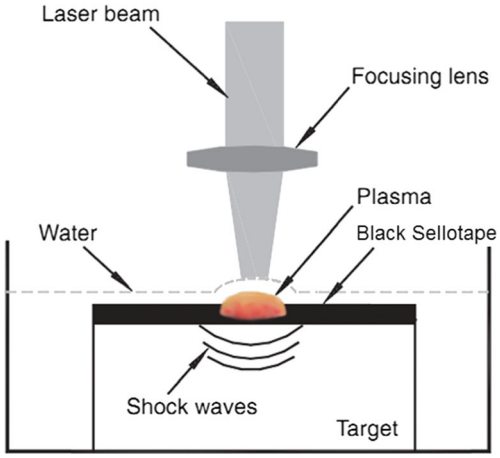


**Fig. 1** Schematic configuration of the LSP process

The LSP procedure has also been applied in the medical field. Sealy and Guo in 2010 tried to solve the problem with corrosion of biodegradable (Mg-Ca) alloy orthopedic implants by applying LSP. The young's modulus of magnesium-based implants such as (Mg-Ca) alloy orthopedic implants mentioned above and that of cancellous bones are similar and close to each other. It can be the reason of minimizing the stress shielding while providing both biocompatibility and adequate mechanical properties. The problem is controlling the corrosion rates of Mg implants so that degradation matches to the bone growth. Therefore, LSP was used as an innovative surface treatment to slow down corrosion rates of novel Mg-Ca implants [5].

Another effort regarding grain refinement using LSP performed by Lu et al. in 2010 revealed that in order to reach a grain size of about 50–200 nm for ANSI 304 stainless steel, multiple laser shock processing has to be applied [6].

Guo and his teammate in 2012 made a study on producing micro dent arrays on titanium alloy surfaces using LSP method. The surface micro dent task could act as lubricant reservoir in order to reduce friction and wear specially in sliding and rolling contact applications. Combination of micro LSP with a CNC mechanism could make an attractive and reliable method for producing micro dent arrays. The surface integrity of samples when subjected to LSP shows a clear enhancement in comparison with alternative methods such as micro machining that presents obvious limitations [7].

Maawad et al. in 2012 investigated laser peening without coating (LPwC) and its effects on the residual stress state and fatigue performance when performing on titanium alloys. The results revealed that the high cycle fatigue performance improved significantly after LPwC [8].

In 2012, H. Lim et al. showed that LSP can be considered as an option for reducing abrasion and corrosion properties of seawater desalination pump parts. In their study, the wear volume and corrosion rate of samples were reduced by 39 and 74.2 %, respectively. Also, the other improvement result after LSP shows that the number and the size of corrosion pits decrease approximately by half when samples are subjected to copper-accelerated acetic acid salt spray test [9].

There are other studies on grain refinement following the LSP process. H. Ding and his partner in 2012 showed, by developing a numerical framework, that in order to achieve a dislocation cell size below 250 nm of monocrystalline copper, a laser energy density of the order of 500 GW/cm$^2$ is necessary [10].

There is another study done in 2013 by Zhang et al. on LSP effects on electromechanical corrosion resistance of weldments. The investigation were carried out by X-ray diffraction (XRD) technique, scanning electron microscopy (SEM), roughness tester, and optical microscopy to see the effect of LSP on corrosion, residual stress, surface roughness grain refinement, and slip. The results revealed that after applying LSP, the erosion and corrosion resistance of samples were improved [11].

In 2013, Kanou et al. performed an analysis of the formation surface layer polycrystalline metals subjected to LSP. The finite-element simulated results revealed that when peening in constant energy, those with bigger spot size will cause to penetrate more strain beneath the surface. But the smaller spot size makes bigger strain just beneath the surface [12].

Generally, in most experiments, the effect of a single parameter such as the laser intensity, irradiance, laser wavelength, laser spots of transparent overlay, overlapping, absorbent coating, laser spot diameter, laser pulse width, and multiple LSP has been considered. However here, when testing different spot diameters, it seems impossible to keep constant the intensity of laser on the surface. Some researchers did not consider relation between parameters and their limitations or even some of them used finite-element simulation to predict desired results. In addition, there is no single way in which how to consider the overlapping of laser spots. In some investigations, the LSP treatment with 30, 50, or even 75 % overlapping were chosen which are the displacement of laser spots relative to their diameters ([8, 12–14]).

**Table 1** Comparison of the chemical composition (%) of ANSI 316L stainless steel and that of samples

| Grade 316L | Fe | C | Mn | Si | P | S | Cr | Mo | Ni | N |
|---|---|---|---|---|---|---|---|---|---|---|
| AISI standard | Base | ≤0.03 | ≤2 | ≤1 | ≤0.045 | ≤0.03 | 16–18 | 2–3 | 10–14 | ≤0.1 |
| Workpiece | Base | 0.016 | 1.5 | 0.47 | 0.02 | <0.001 | 17.21 | 2.14 | 10.44 | – |

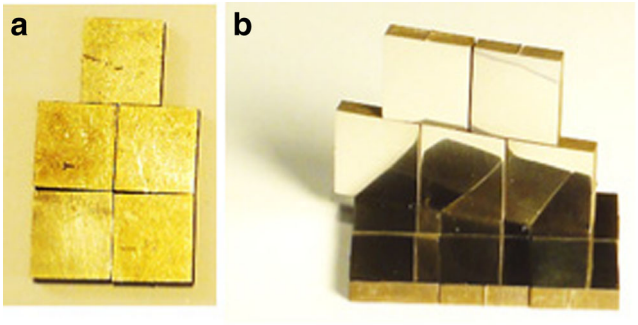


**Fig. 2** Samples **a** before and **b** after surface polishing

The authors believe that converting of displacement percentage or overlapping amount of pulse spacing to a factor called average numbers of peening (ANP) which we will come back to it can result a better understanding of their effects.

In this study, we used an advanced design of experience using MATLAB to overcome the problems which just mentioned, so the effects of all input parameters on the results can be seen individually.

## 2 Experimental procedure

(a) Sample preparation

The material of our sample is a 316L stainless steel and according to AISI standard, chemical composition of that is shown in Table 1.

In order to compare the hardness and corrosion behaviors, it is needed to have very similar sample characters (such as area, dimensions, and surface roughness); hence, the samples were cut precisely using wirecut into rectangular shapes with dimensions of $10 \times 10 \times 3$ mm$^3$ (width × length × thickness) and polished up to the mesh 3000. Figure 2 shows the samples (A) before and (B) after surface finishing.

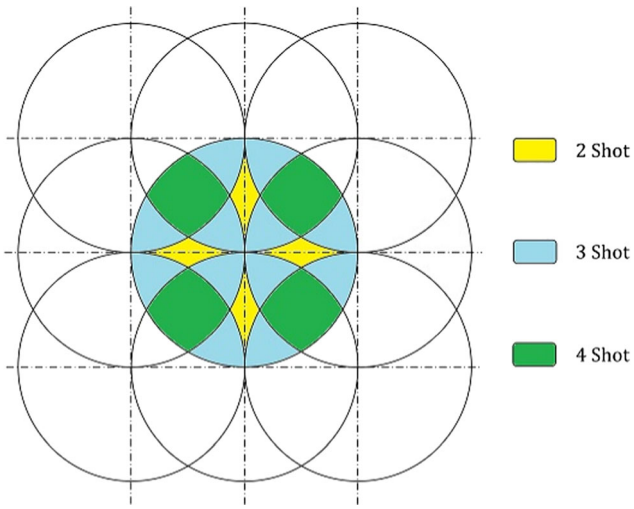


**Fig. 3** The number of shot impacts to the different areas of spot

**Table 2** The ANP and the related overlapping percentage of diameter

| Overlapping percentage of diameter | 25 % | 50 % | 60 % | 75 % |
|---|---|---|---|---|
| ANP | 1.5771 | 3.2907 | 5.1172 | 12.6455 |

Before applying the LSP technique, the workpiece's surface has to be covered by two layers. The first one is the absorbent coating which its main task is to protect the workpiece surface from thermal effects of the generated plasma [1], resulting in more refinement in near surface stress distribution and the suitable material for this purpose which was tested is black sellotape. The second one is the transparent overlay, where its job is confining of the plasma and therefore increasing plasma pressure in the vicinity of the workpiece's surface and deionized (DI) water is most convenient transparent material. The magnitude of generated plasma pressure is the reason for severe plastic deformation, micro structural changes, increasing dislocation, and grain refinement near the surface, and their quantities reduce by penetrating through the depth.

No other processing is required for preparing samples for micro hardness testing after LSP. But in electrochemical testing, the samples should be prepared as working electrodes. The electrochemical cell consists of three electrodes and a 3.5 % sodium chloride (NaCl) solution was used as electrolyte.

(b) Design of experiment

In the current work, as far as we are limited to inherent limitation of inputs combination of laser system, we could not meet all the requirements for investigating a single parameter thoroughly. In the other word, it is not possible to design a full factorial experiment to identify all the conditions by the input value ranges, and those system limitations force us to choose limited combination of inputs for LSP.

Design of experiment is performed to reduce the number of tests and more importantly to overcome the system limitations to expand results to the region where experiment cannot cover. So, engineered inputs are proposed by mean of D-optimal design method. To this aim, we should first introduce a new parameter which we call it "Average Number of Peening" (ANP) described in Eq. (1) as follows:

$$ANP = \sum_1^n n_i a_i \Big/ \sum_1^n a_i \tag{1}$$

**Table 3** The laser system specifications used for applying LSP

| Diameter of laser spot | Pulse shape | Repetition rate | Pulse duration time | Wavelength | Energy/pulse | Laser type |
|---|---|---|---|---|---|---|
| ~7 mm | Gaussian TEM 00 | 1–10 Hz | 5 ns | First harmonic 1064 nm | 0.32–0.58 Joule | Nd:YAG Q-switched |

Where $n_i$ is the number of shots on the specific area ($a_1$) (Fig. 3).

The D-optimal design is one of the predefined methods for design of experiment in MATLAB software. The D-optimal method takes the inputs such as ANP, laser intensity, laser spot size, and number of experiments and gives back the best combination of them to minimize errors of approximation for expanding results. This method is also useful to analyze parametric influence of process factors on responses. The results of optimized inputs and all 14 consequent outputs are shown in both Tables 6 and 7.

Table 2 shows the ANP and the related overlapping percentage of diameter so by converting conventional input methods such as the type of overlapping into numerical and defined method like ANP, we are able to have a better understanding of the LSP effects.

(c) Experimental setup

System requirements for applying LSP technique include an Nd:YAG pulsed laser system with suitable wavelength and pulse width.

Laser's energy should provide the required intensity in the range of GW/cm$^2$ according to the laser spot size. Other studies showed that choosing such a laser system provides pressures in the range of GPa which can produce high strain at high strain rates. The laser system specifications used in this study are shown in detail in Table 3.

Selected parameters for micro hardening machine and for electrochemical testing are shown in Tables 4 and 5, respectively.

Two methods of electrochemical testing including Tafel (Linear) test and Nyquist (FRA[1]) were performed.

The LSP setup consists of a laser system, focal lenses, workpiece, driving table, and water container which are schematically shown in Fig. 4.

The focused laser beam passes through DI water (as a rather transparent overlay) and reaches the absorbent coating. When a laser pulse with sufficient intensity impacts the absorbent coating, the material vaporizes and converts to plasma.

The plasma absorbs most of the laser energy, so the fast expanding plasma is trapped between the surface of workpiece and the transparent overlay, which both are confining the generated plasma, causes a high plasma pressure that propagates into the material as a shock-wave. After the first shot, the sample is moved by driving table to the pre-defined position of the next shot.

[1] Frequency Response Analyzer

## 3 Results and discussion

In this paper, the experiment is designed by D-optimal algorithm of MATLAB with respect to the primary test design limitations. Therefore, the effects of all input parameters on the results can be seen individually. A D-optimal design is performed to choose the best input parameters in order to overcome the limitations of the testing area, which is generated by an iterative search algorithm and seeks to minimize the covariance of the parameters for a specified model. Inputs of the process are consisted of laser intensity, laser spot size, and the ANP and our investigation seeks micro hardness and electrochemical enhancement.

### 3.1 Micro hardness testing and analysis

The results of micro hardness testing are shown in Table 6. Where SD is the laser spot diameter, $I$ is laser intensity, $d_1$ and $d_2$ are the average of smaller and larger diameters of pyramid base of micro Vickers testing, respectively, $HV_1$ shows the measured hardness and, CI is the confidence interval of hardness measurements and finally $\alpha$ shows the gradient distribution of hardness which is defined as follows:

$$\alpha = \frac{d_2 - d_1}{d_2 + d_1} \times 1000 \tag{2}$$

One of the main reason for the gradient distribution of results ($\alpha$) is non-uniformity of laser profile (e.g., Gaussian). In order to obtain a better understanding of laser input effects, the experimental results are sorted by laser intensity and the ANP (Eq. 1) which are shown in Fig. 5. As it is seen by increasing the laser intensity, the gradient of hardness distribution is increased, where it cannot be

**Table 4** The selected parameters for micro hardening measurements

| | |
|---|---|
| Applied force | 9.807 N |
| Dwell time | 10 s |

**Table 5** The parameters for two electrochemical testing methods, (Tafel and Nyquist)

| | | |
|---|---|---|
| Tafel (Linear) | Potential range | −0.25 to +0.25 V |
| | Step height | 1 mV |
| | Scan rate | 1 or 10 mV/S |
| | Initial open circuit delay (OPC) | 60 s |
| FRA (Nyquist) | FRA method | Single sine [SS] |
| | Initial open circuit delay (OPC) | 1000 s |
| | Frequency range | 10 mHz–10 kHz |

concluded such a result by considering the ANP. So analyzing the processed inputs such as the ANP and laser spot size held to the MATLAB. The MATLAB analyzing results for the gradient of hardness distribution is shown in Fig. 6.

Figure 6 shows that by increasing SD (laser spot size) and decreasing ANP, the gradient of hardness distribution (inhomogeneity or $\alpha$) is increased. Decreasing in homogeneity of hardness distribution ($\alpha$ is enhancing) is normal when laser intensity is increased as Fig. 5 shows.

According to Kanou's work [12] and Ding's study [1] for large spot size, the strain propagates like a planar front, which attenuated at a rate of 1/r ($r$ = radius of spot), while for smaller spot sizes, strain expands like a sphere which attenuated at a rate of $1/r^2$. Hence, peening with larger spots leads to deeper strain beneath the surface while peening with smaller spots leads to more overlapping of impulses just beneath the surface. The advantage of overlapping for smaller spots is that it compensates some of the remaining untreated areas due to damping effect. Damping comes from multiple reasons such as the mismatching effects of the layers, shock smoothing due

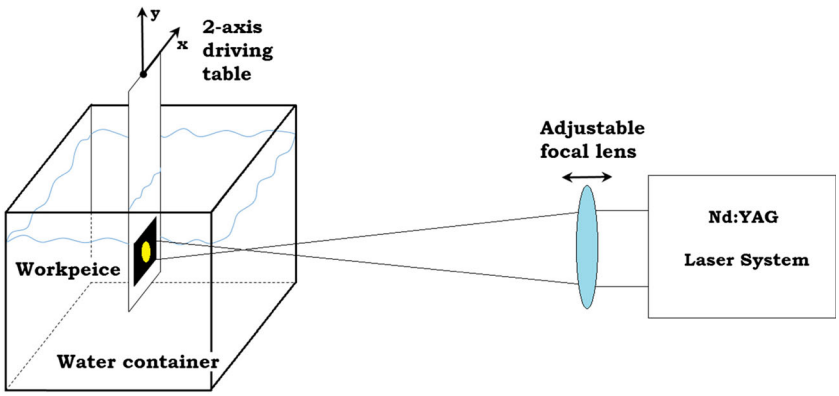


**Fig. 4** The schematic of LSP setup

**Table 6** Micro hardness testing results of ANSI 316L stainless steel after LSP shows the gradient distribution of hardness and HV

| Number | CI | HV1 | $\alpha$ | $d_{2[\mu m]}$ | $d_{1[\mu m]}$ | $ANP_{[count]}$ | $I_{[GW/cm^2]}$ | $SD_{[mm]}$ |
|---|---|---|---|---|---|---|---|---|
| Untreated | 1.15 | 158.2 | 6.5 | 109 | 107.6 | – | – | – |
| 1 | 0.45 | 164.0 | 2.82 | 106.6 | 106.0 | 3.3 | 3.7 | 2 |
| 2 | 1.02 | 168.4 | 5.72 | 105.5 | 104.3 | 6.6 | ″ | ″ |
| 3 | 0.91 | 164.8 | 4.71 | 106.6 | 105.6 | 26.4 | ″ | ″ |
| 4 | 0.46 | 164.0 | 2.82 | 106.6 | 106.0 | 52.8 | ″ | ″ |
| 5 | 1.16 | 169.6 | 5.26 | 105.1 | 104.0 | 26.4 | 6 | 1.3 |
| 6 | 0.63 | 167.6 | 4.28 | 105.6 | 104.7 | 3.3 | 10 | 1 |
| 7 | 0.18 | 169.0 | 4.77 | 105.3 | 104.3 | 6.6 | ″ | ″ |
| 8 | 0.53 | 168.2 | 3.81 | 105.4 | 104.6 | 13.2 | ″ | ″ |
| 9 | 0.76 | 167.7 | 3.33 | 105.5 | 104.8 | 26.4 | ″ | ″ |
| 10 | 0.21 | 166.9 | 3.79 | 105.8 | 105.0 | 52.8 | ″ | ″ |
| 11 | 1.17 | 168.0 | 6.18 | 105.8 | 104.5 | 3.3 | 100 | 0.3 |
| 12 | 0.84 | 166.9 | 5.22 | 106.0 | 104.9 | 13.2 | ″ | ″ |
| 13 | 0.43 | 166.9 | 8.53 | 106.4 | 104.6 | 26.4 | ″ | ″ |
| 14 | 1.07 | 165.6 | 5.68 | 106.3 | 105.1 | 52.8 | ″ | ″ |

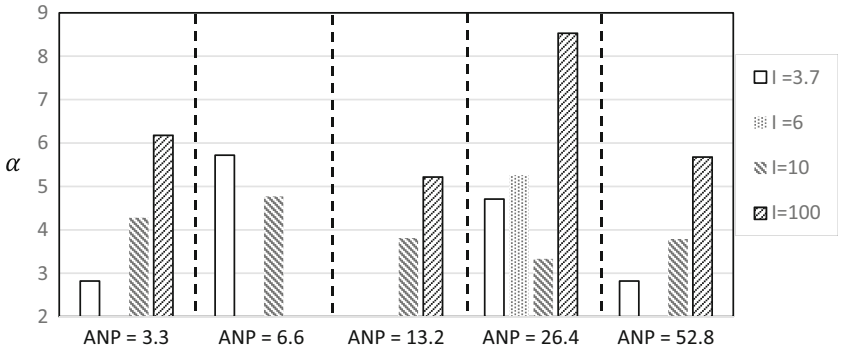


**Fig. 5** Inhomogeneity of the hardness distribution with respect to laser intensity (GW/cm$^2$) and the ANP

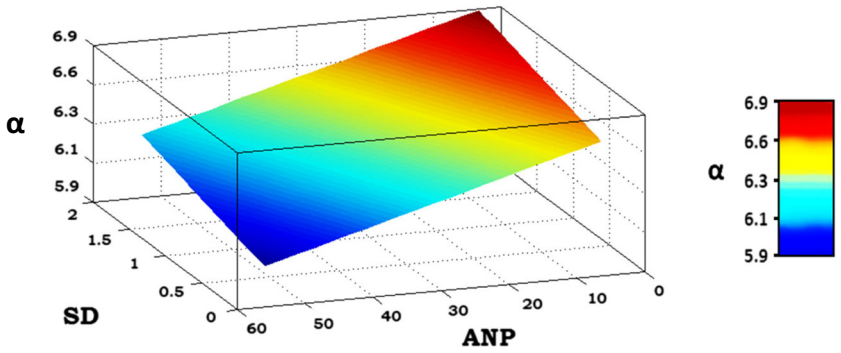


**Fig. 6** The gradient of hardness distribution thorough the workpiece for constant intensity ($I = 100$ GW/cm$^2$)

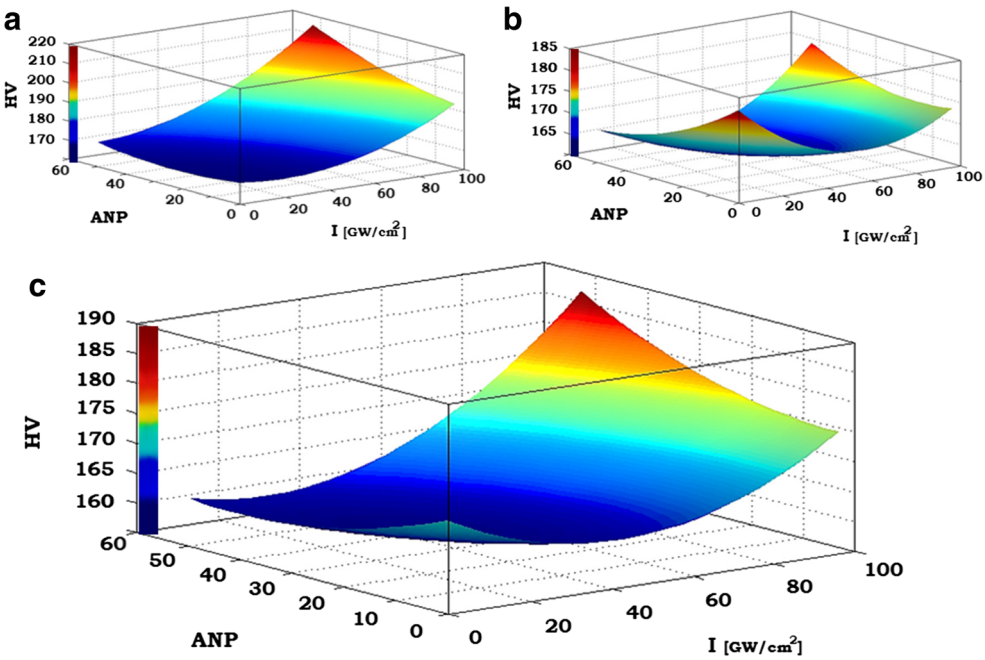


**Fig. 7** The effects of laser intensity and ANP on hardening with different spot size. **a** 2 mm, **b** 0.3 mm, and **c** 1 mm

**Table 7** Corrosion resistance (Z) of Nyquist testing

| Sample | $Z_{[\Omega cm^2]}$ | $ANP_{[count]}$ | $I_{[GW/cm^2]}$ | $SD_{[mm]}$ |
|---|---|---|---|---|
| Untreated | 48395.5 | – | – | – |
| 1 | 55638.38 | 3.3 | 3.7 | 2 |
| 2 | 81104.63 | 6.6 | ″ | ″ |
| 3 | 68396.31 | 26.4 | ″ | ″ |
| 4 | 55352.19 | 52.8 | ″ | ″ |
| 5 | 67411.31 | 26.4 | 6 | 1.3 |
| 6 | 52788.88 | 3.3 | 10 | 1 |
| 7 | 82957.38 | 6.6 | ″ | ″ |
| 8 | 58493.06 | 13.2 | ″ | ″ |
| 9 | 82659.25 | 26.4 | ″ | ″ |
| 10 | 63745.76 | 52.8 | ″ | ″ |
| 11 | 62072.88 | 3.3 | 100 | 0.3 |
| 12 | 68544.81 | 13.2 | ″ | ″ |
| 13 | 58395.75 | 26.4 | ″ | ″ |
| 14 | 54183.31 | 52.8 | ″ | ″ |

to passing the absorbent layer, and impulse intensity threshold for hardness effect [1].

The damping phenomenon decreases peening efficiency by reducing the effective surface of peening. Hence, because of peening geometry in most LSP works, damping leads to less homogeneous samples.

Since the larger spots could not compensate the damping effect by more overlapping of impulses which comes from spot size and its relation with strain propagation, the target encounters with more untreated gap between pulses. That is how bigger spot size causing less homogeneity in results.

Our improvement is supposed to have more homogeneous results when the ANP is increased, owing to the cold working. This means that when applying strain to the workpiece for the first time, it is much easier to form the substance, compared to the case when it has already been formed. In the other hand, the substance is getting close to its saturating point for cold working. So, increasing the ANP should cause of more homogeneity in results (Fig. 6).

Generation of water pollution and nanoparticles as a result of laser ablation causes quality loss of transparent overlay and quality loss of impulses that is reducing efficiency of the processing consequently. Thus, the resulting hardness also decays through the process due to the pollution. It means that in the beginning of the process, according to the inputs, the sample hardness decays a bit and then starts growing. Micro hardness analysis of the LSP process is shown in Fig. 7.

According to Fig. 7, as the laser intensity and the ANP increase, the hardness of samples is varied as a quadratic function. From Fig. 7b, c, it is ascertained that the hardness of samples firstly decreases and then increases by increase in I or/and ANP. It seems that at the low intensity or/and ANP, the effect of the existence of pollution is dominated whereas at high intensity or/and high ANP, the effect of laser intensity and the magnitude of ANP are dominated. It should be mentioned that, the laser spot size, directly effects on variation of hardness of samples, large spot size results in a better hardening results, when the smaller spots cause more pollution in water. Increasing the laser spot size (Fig. 7a) results in less pollution in the transparent layer and larger hardness is more likely. Finally, however, the direct results show that the enhancement of about 11 micro Vickers's units (7 %), but the MATLAB analyzed result offers 34 % improvement (56.8 units) for the best combination of input values.

### 3.2 Electrochemical tests and analysis

The electrochemical test results are shown in Table 7 in which the introduced experimentally designed factors are inputs for Nyquist inspection in the electrochemical tests. The system which were used is EG&G system.

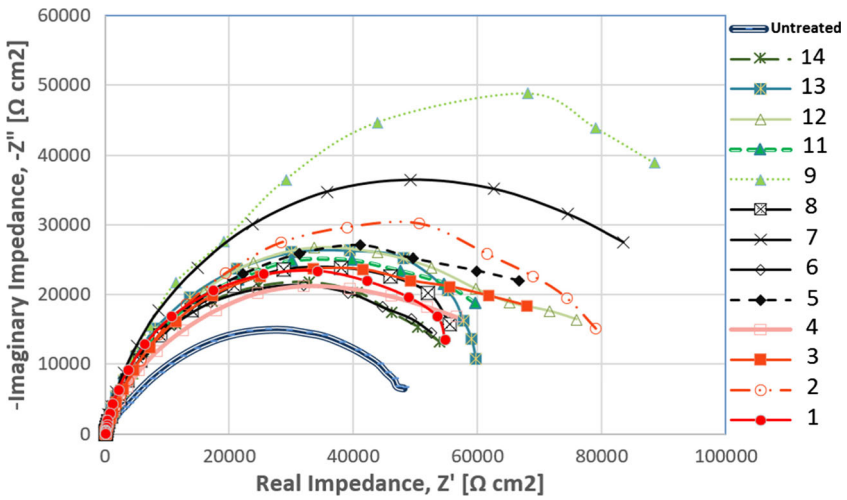


**Fig. 8** The diagram of Nyquist results and corrosion resistance of the ANSI 316L

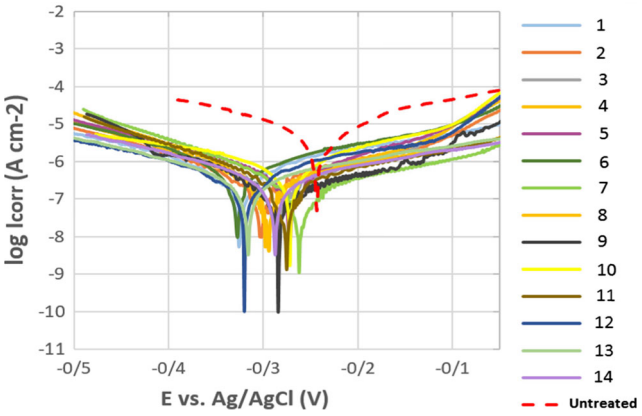


**Fig. 9** The curves of Tafel and corrosion features of lased peened samples of 316L stainless steel

Table 7 shows enhancement of corrosion resistance for all samples compared with that of the untreated sample. The diagram of Nyquist tests is also shown in Fig. 8. It should be mentioned that the electrochemical system which was used is a system with three electrodes and the NaCl 3.5 % solution was used as electrolyte.

The other electrochemical test is Tafel test that measures the potential and current of the corrosion of 14 different samples with specific features that revealed in Table 5 (Fig. 9).

It is obvious that curve numbers in Figs. 8 and 9 are related to the numbers of Table 7. According to Fig. 9, the slopes of Tafel curves remain unchanged compared with that of untreated one. It means that corrosion mechanism also remains unchanged and inhibitor plays a roll like coating. The little shift to the negative potential does not mean the corrosion mechanism is shifted to cathodic inhibitor, since cathodic inhibitor is introduced when there is a variation on the condition of solution and cathode (auxiliary cathode).

So according to the range of the difference in the corrosion potential of other samples it could be ignored this little cathodic shift. But the point is the reduction of corrosion current (corrosion resistance enhancement) of peened samples in this test.

Comparing the result of corrosion tests (Fig. 10) with the hardness results which were shown in Fig. 7, a similarity between them is observed. Figure 10 also shows the effect of some parameters such as laser intensity, ANP, and laser spot size on electrochemical corrosion.

According to this figure, it is inferred that by increase in the values of laser intensity, the ANP, and the spot size, the corrosion resistance is also increased. It should be mentioned that the pollution of environment of LSP and change in the properties of absorbent layer has also same effect on the corrosion as it is on the hardness.

It is clear from the Figs. 9 and 10 that the corrosion is more sensitive to ANP than hardness whereas the hardness is sensitive to the laser intensity compare with the corrosion. Thus, it is inferred that if the aim is the hardness, it is better to increase the intensity of the laser and if the corrosion resistance is the purpose, increasing the ANP is recommending. Of course enhancing the laser spot size is confirmed for both corrosion and hardness tests.

At last in direct corrosion results however it shows an average of 30 % enhancement on corrosion resistance and could be reached to its highest value of 70 %, but the MATLAB analyzed result offers of a little more than 2× improvement for the best combination of input values.

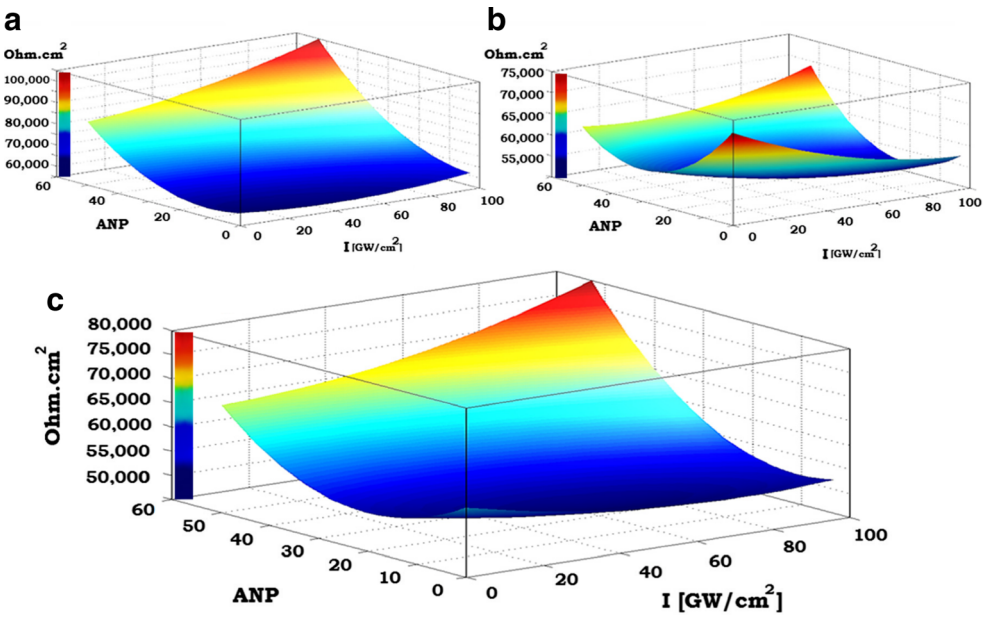


**Fig. 10** The effect of parameters laser intensity, the average number of peening, and the diameter of spot size on electrochemical corrosion with spot laser diameter. **a** 2 mm. **b** 0.3 mm. **c** 1 mm

## 4 Conclusion

The present paper has evaluated the effect of impact size and the ANP and also intensity of impacts on corrosion and hardness properties of 316L stainless steel subjected to LSP. For this purpose, D-optimal design of experiment in Matlab was utilized to predict the results for unallowable inputs combination due to overcome the system limitations and expanding results. The obtained results can be summarized as follows:

(1) Both of corrosion resistance and surface hardness are improved due to increasing of the laser intensity, the ANP, and the laser spot size. Comparing to the untreated samples, surface hardness is enhanced of about 35 % while the corrosion results show the improvement of about 100 %.
(2) The hardness is strongly related to the laser intensity whereas the most effective parameter for corrosion resistance improvement is the ANP.
(3) The LSP does not change the corrosive mechanism, because it does not change the corrosive potential or the slopes of Tafel curves. But reduction of corrosive current means that applying the LSP acts as a coating, which it conducts to improvement of corrosion resistance.
(4) The larger spot size can lead to more anisotropic hardness results. Utilizing proper absorbent coating can result in better distribution of effects in order to more homogenous results.

## References


1. Ding K, Ye L (2006) Laser shock peening, performance and process simulation. Woodhead Publishing Limited "CAMBRIDGE", Boca Raton
2. Warren A, Guo Y, Chen S (2008) Massive parallel laser shock peening: simulation, analysis, and validation. Int J Fatigue 30: 188–197
3. Vukelic S, Kysar JW, Lawrence Yao Y (2009) Grain boundary response of aluminum bicrystal under micro scale laser shock peening. Int J Solids Struct 46:3323–3335
4. Hatamleh O (2009) A comprehensive investigation on the effects of laser and shot peening on fatigue crack growth in friction stir welded AA 2195 joints. Int J Fatigue 31:974–988
5. Sealy M, Guo Y (2010) Surface integrity and process mechanics of laser shock peening of novel biodegradable magnesium–calcium (Mg–Ca) alloy. J Mech Behav Biomed Mater 3:448–496
6. Lu J, Luo K, Zhang Y, Sun G, Gu Y, Zhou J, Ren X, Zhang X, Zhang L, Chen K, Cui C, Jiang Y, Feng A, Zhang L (2010) Grain refinement mechanism of multiple laser shock processing impacts on ANSI 304 stainless steel. Acta Mater 58:5354–5362
7. Guo Y, Caslaru R (2011) Fabrication and characterization of micro dent arrays produced by laser shock peening on titanium Ti–6Al–4V surfaces. J Mater Process Technol 211:729–736
8. Maawad E, Sano Y, Wagner L, Brokmeier H-G, Genzel C (2012) Investigation of laser shock peening effects on residual stress state and fatigue performance of titanium alloys. Mater Sci Eng A 536: 82–91
9. Lim H, Kim P, Jeong H, Jeong S (2012) Enhancement of abrasion and corrosion resistance of duplex stainless steel by laser shock peening. J Mater Process Technol 212:1347–1354
10. Ding H, Shin YC (2012) Dislocation density-based modeling of subsurface grain refinement with laser-induced shock compression. Comput Mater Sci 53:79–88
11. Zhang L, Zhang Y, Lu J, Dai F, Feng A, Luo K, Zhong J, Wang Q, Luo M, Qi H (2013) Effects of laser shock processing on electrochemical corrosion resistance of ANSI 304 stainless steel weldments after cavitation erosion. Corros Sci 66:5–13
12. Kanou S, Nishikawa M, Soyama H (2013) Analysis of the formation of plastic deformation layer on the surface of polycrystalline metals subjected to a micro-size high-rate shot impact. Int J Mech Sci 75:316–323
13. Dorman M, Toparli M, Smyth N, Cini A, Fitzpatrick M, Irving P (2012) Effect of laser shock peening on residual stress and fatigue life of clad 2024 aluminium sheet containing scribe defects. Mater Sci Eng A 548:142–151
14. Brockman RA, Braisted WR, Olson SE, Tenaglia RD, Clauer AH, Langer K, Shepard MJ (2012) Prediction and characterization of residual stresses from laser shock peening. Int J Fatigue 36:96–108